Simulation, testing and implementation of temperature-reduction solutions on a high-power thermal demonstrator

Andy Heinig[1], Dimitrios Papaioannou[1],
[1] Fraunhofer Institute for Integrated Circuits, Design Automation Division, Zeunerstraße 38, 01069, Dresden, Germany
Email: firstname.lastname@eas.iis.fraunhofer.de

ABSTRACT

High-power applications in microelectronic devices and systems is a crucial and severe issue that may cause elevated thermal and thermomechanical phenomena and finally lead the fabricated system to degradation, limitation of its performance, or even failure and destruction of its features. In specific applications, such as those found in the industry and the automotive sector, the power produced by the components may reach 50W or even higher, leading to extreme temperatures in the electronics and mechanics parts. On one hand, the integrated circuits must be able to function properly under such elevated temperatures; on the other hand effective cooling solutions, including heat-sinks, heat-spreaders, thermal interface materials, fans, etc., must be implemented. Their primal role is to remove the major part of the dissipated heat to the environment (usually air), without severely affecting the performance of the included electronic components. Such phenomena and effects can be studied prior to device and system fabrication and their behavior and influence may be depicted and analyzed thanks to design and multiphysics finite elements simulation programs; this procedure is usually time- and cost-saving, since the software tools help us discover, remove or limit major undesired issues. However, the modeling and simulation procedures require that the necessary simplification and modeling guidelines will be applied, the right material properties will be given and the appropriate boundary conditions (such as coefficient of thermal expansion, the thermal conductivity, heat capacity, etc.) will be set. We built a high-power thermal demonstrator consisting of several heat-sources and resistors, placed on a standard PCB (printed circuit board); it functions under several Watts power, up to 35 W. On one hand, we modeled and simulated the behavior of the system with respect to the induced power and the temperature found inside the system. For that purpose, we implemented several NTC (negative temperature coefficient) resistors serving as reference points for the temperature measurements of the demonstrator. On the other hand, we managed to reduce the temperature of the test-system by applying several TIM (thermal interface materials) and a set-up including a fan and a heat-sink for high-power applications. Various simulation and test cases under different flow and power conditions have been investigated and their results have been compared. Moreover, a very good numerical proximity between the simulations and the results obtained from the actual test measurements have been found. Finally, the system has been proved stable and was able to operate after several thermal cycles under 40W without any troubleshoots.

KEY WORDS: thermal demonstrator, high-power, thermal phenomena, finite element simulations, test-system, thermal measurements, heat-sink, thermal interface materials, cooling solution, temperature reduction

NOMENCLATURE

TIM	thermal interface material
NTC	negative temperature coefficient
FR-4	flame retardant
CP	chip power
PCB	printed circuit board
FEM	finite element method
T/ T_{max}	temperature/ maximum temperature
R	resistance
IC	integrated circuit
MEMS	micro-electro-mechanical system
FPGA	field programmable gate array
Si	silicon
Cu	copper
Al	aluminum
h_c	convective heat transfer coefficient (W/m^2*K)
k	thermal conductivity (W/m*K)
Q	rate of heat transfer (W/m^3)
q	conductive heat-flux (W/m^2)
C_p	heat capacity (J/kg*K)

Greek symbols

ρ	mass density (kg/m^3)

INTRODUCTION

All the electronic and microelectronic systems, from the smallest ones to the largest and most complicated ones show thermal and thermomechanical natural effects and phenomena caused by power dissipation, such as temperature elevation of the components, volume expansion and thermomechanical stresses, etc. They affect the performance, life-span, durability, robustness and reliability of the fabricated products where they are incorporated in. High temperatures and heated components are responsible for the majority of troubleshoots, defects and failures in electronic and microelectronic devices and products. [1, 2]

If we want to explore in more detail the components that are responsible for the heat production and temperature elevation inside the microelectronic systems, we would start with the various ICs and the complex logical functions they perform. Their degree of integration and complication increases the influence of thermal and thermomechanical phenomena. Systems with small dimensions are always desired in microelectronics, but their heat is dissipated in a narrower and more limited space, leading to higher temperatures and stresses. Moreover, in systems with smaller dimensions it is more difficult to implement cooling solutions such as heat-sinks, because they are usually bulky structures. For example, in 2.5D and 3D interposer-based architectures, the various components (Systems-in-package, MEMS, FPGAs, memories, etc.) are either forming vertical stacks or are placed side-by-side. Due to power produced by the stacks of ICs, severe and intense thermal and thermomechanical phenomena arise in the system, where interposer offers an additional mechanism for better temperature distribution and dissipation. However, the kind of specific applications that every microelectronic system if used for, plays a significant role and dictates the degree of produced heat and thus the influence of the thermal effects: there are systems that operate under several mW of power and other complex industrial ones that work under several hundred W. [1-10]

The power dissipation in microelectronics is always accompanied with a lesser or greater increase of temperature; the components heat up and their volume is increased. In this case, material properties, such as the thermal conductivity k, the heat capacity C_p and the coefficient of thermal expansion CTE play an important role. Due to CTE-mismatches crucial and severe effects and deformations may emerge, especially when the materials in contact have significant difference in their CTEs: for examples, metals and plastic molds. Such intense phenomena may lead to ruptures, defects, cracks or failures in the features due to high thermomechanical stresses. Subsequently, this may affect the reliability, robustness and performance of the systems. [1-12]

In order to effectively optimize the heat dissipation, reduce the thermomechanical stresses and improve the thermal performance of the systems, several temperature-reduction solutions can be implemented: thermal interface materials (TIMs) of various forms and dimensions (e.g. glue epoxies, gap filler pads, etc.), heat sinks of various materials and shapes (e.g. with pins, or fins, made of copper or aluminum), heat spreaders, axial cooling fans and coolers depending on the applications, requirements and specifications of the system can be added. [11-12, 20]

Thermal interface materials are specific materials with very good thermal properties that are placed on the heat-generating components of the system, such as the ICs. They are always used in combination with a heat-spreader or a heat-sink placed on top of them. If the metal surface of the heat sink is in direct contact with a die, the air gaps between the two surfaces wouldn't let the heat properly dissipate through the heat-sink due to the surface roughness. The TIMs are flexible and compressible materials, softer than metals or plastics; by pressing them between the heat-sink and the dies, they cover the gaps between the two surfaces and optimize the part of the heat that is dissipated through the heat-sink. Hence, they reduce the heat part that is dissipated through the PCB and other important components of the system. As a result, these components have lower temperatures, limited thermomechanical stresses and better thermal behavior and performance. [11-12]

Finite-Element-Method-based (FEM) simulations is a very useful tool in order to investigate the multiphysical behavior of modeled components and systems and avoid troubleshoots, problematic issues and failures prior to their actual fabrication, a process that is time-consuming and costly. With FEM software tools we can model the desired systems, achieve reliable, fast and accurate results, extract graphical representations, illustration, numerical arrays, etc. Furthermore, simplification models and concepts can be implemented in order to reduce the degree of complexity and simulation time of the modeled systems. Hence, we can achieve results that are close to the expected ones and predict the behavior of the system and avoid possible failures and severe issues. [3, 6, 7, 9, 10]

Microelectronic demonstrators are test-systems that incorporate various microelectronic components (e.g. CMOS, Systems-in-package, FPGAs, resistors, capacitors, etc.) found in most of the cases on a standard PCB board and connected with power, ground and other devices (e.g. for external measurements, such as oscilloscopes and multimeters). The thermal test-system focus on the investigation of the thermal behavior of the various components.

In the current paper we present and investigate the thermal behavior of a microelectronic demonstrator under high-power applications (up to 40W approximately), before and after several concrete components for temperature reduction were applied. For that purpose we implemented two thermal interface materials (a soft and flexible gap filler pads, combined with an adhesive film), a heat-sink and a DC axial fan. The initial test-system consists of a standard PCB board, where several CP power resistors and multilayer NTC resistors are arranged on its surface: the first ones are used as heat-sources and the latter ones as the reference elements, whose temperature values are measured and compared with the numerical results extracted from the simulations for various test-cases. Finally, we try to predict how the system behaves under 50W and 100W of applied power with the aforementioned cooling components added to the system.

Figure 1 shows the fabricated high-power thermal demonstrator before the heat-sink, TIMs and axial DC fan were implemented. Figure 2 shows the designed version of the thermal demonstrator used during the simulations.

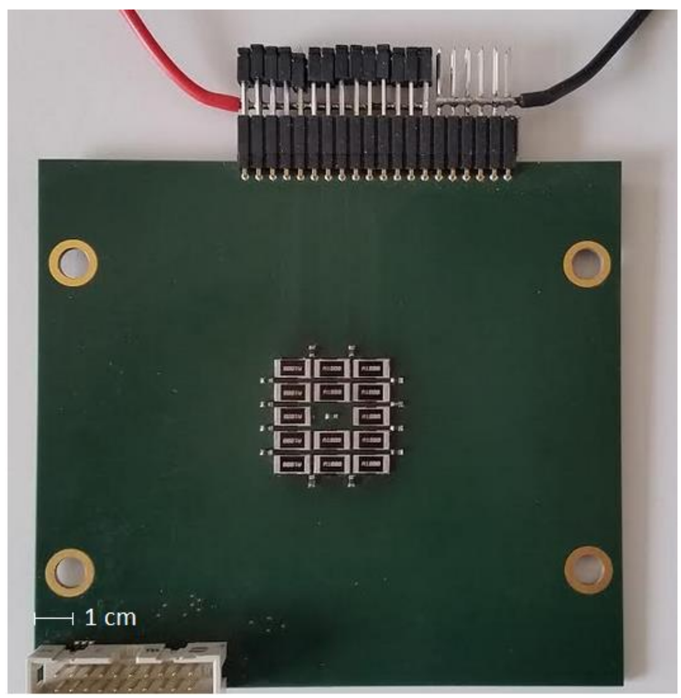

Fig. 1 The main components of the fabricated thermal demonstrator are 14 CP power resistors and 13 NTC thermistors; they are placed on a standard PCB board.

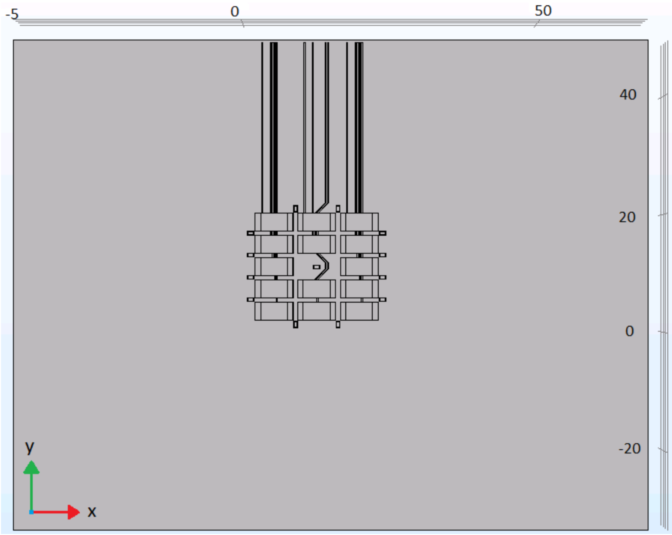

Fig. 2 The designed model of the thermal demonstrator

DESCRIPTION OF THE DEMONSTRATOR

System components

The fabricated high-power thermal test-demonstrator is a simple structure and its main components are two different sorts of resistors: 13 chip power CP series resistors (CPA2512 type) that can function up to 155 ºC and used as heat-sources and 14 multilayer NTC thermistors (ERTJ1VS type for temperature control) that we used as reference structures for the comparison of the temperature values between the simulations and the actual experimental measurements, as mentioned above. [14, 15]

The 27 resistors were placed on a standard PCB board that consists of a top and bottom layer of copper tracks and an insulating FR-4 layer in the middle. The board has 106 mm length and 82 mm width and the copper tracks have 35 μm thickness and 100 μm width. Finally, an array of pin connectors was used for the connection of the system with a power-source, the ground and for the measurement of the electrical resistance of the NTCs. Concerning the dimensions of the main components: the CP power resistors have 6.3 mm average length, 3 mm average width and 0.7 mm average height. The NTCs are smaller and have 1.1 mm average length, 0.5 mm average width and 0.8 mm average height. The overall active area of the demonstrator (the array of NTCs and CP resistors) is approximately 22x20 mm (LxW); however the PCB where they are mounted on is much larger, as mentioned above. [14, 15]

Figure 3 gives a closer look to the active area of the thermal demonstrator. The NTCs are the small resistors placed on the top, bottom, left, right and central are of the design. The CP series resistors are bigger and bring the A1000 mark. The etched lines show the copper tracks on the PCB board used for the signal transmission. [14, 15]

After the fabrication of the demonstrator, we connected it with the power-source and we used a digital multimeter in order to measure the electrical resistances of the 13 NTCs and translate their R-values into temperature values (based on the R-T diagram provided by the manufacturer). By regulating the voltage and current supplied by the power-source to the CP resistors of the demonstrator, we managed to apply the desired power: 1W-7W before the implementation of the temperature-reduction components and 1W-35W afterwards. The natural relationship between the resistance of the NTCs and the temperature of an resistor is that its R decreases with increasing applied power: at 25 ºC, the R is 100 KΩ, at 50 ºC, its R is 32.5 KΩ at 75 ºC, its R is approx. 12 KΩ. [14, 15]

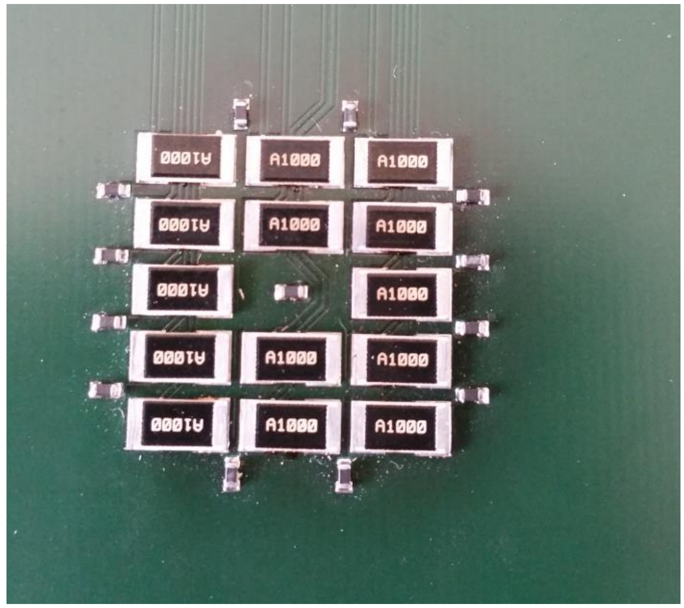

Fig. 3 Detailed view of the active area of the thermal demonstrator that includes the CP resistors and NTC thermistors.

Parallel to the conduction of the experimental measurements and processing of the results, we modeled and simulated the test-system. No simplifications concepts were implemented in order to achieve a very good proximity between the modeled and the actual system. Figure 4 shows a closer view to the active area of the modeled system.

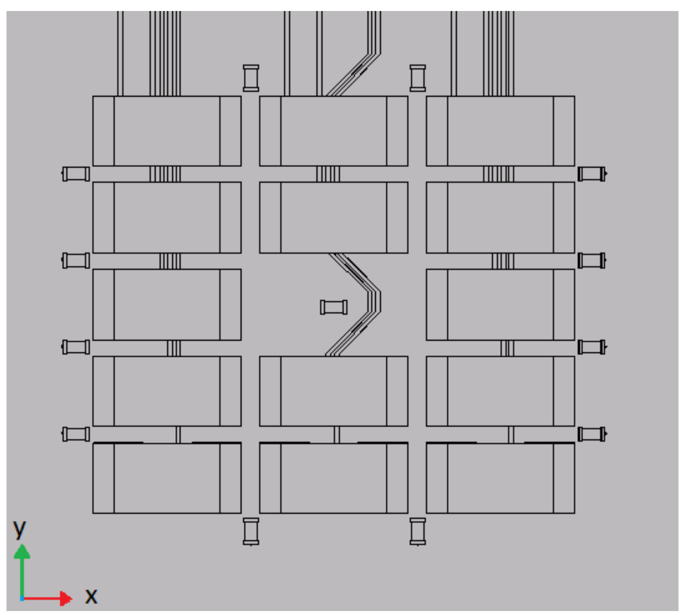

Fig. 4 Closer view to modeled area with the CP power resistors and the NTC thermistors of the thermal demonstrator.

Description of the cooling components used for better thermal performance

After the completion of the simulations and experimental measurements of the system under 1W-7W, we added the heat-sink, two different TIMs (placed between the heat-sink and the CP resistors) and a DC axial fan in order to improve the heat dissipation of the system, reduce its overall temperature values of the components and achieve power applications up to 40 W approximately.

The heat-sink (model number R23, manufactured by 'Dynatron') has dimensions 106x82x62 mm (LxWxH) and it is made of aluminum, a material with excellent thermal properties (its thermal conductivity is approximately 238 W/m*K). By adding the heat-sink we ensured that the heat is primarily dissipated through it and subsequently through the ambient air. Hence, the part of the heat that dissipated to the resistors and the PCB is much lower. This model of heat-sink can support application up to 135 W and for our cooling purposes it was mounted with screws and bolts on top of the CP resistors and NTC thermistors. Finally, concerning its structure, it consists of a thin base, where 35 vertical fins are attached to it. [23]

Between the heat-sink and the resistors/NTCs two different TIMs were placed: the first one is a gap filler pad ('thermal interface superthermal D089 pad' manufactured by Aavid) and the second TIM is an adhesive film (ceramic filled adhesive film). The first is soft with excellent thermal properties (its thermal conductivity k is 8.9 W/m*K) and the other is a hard adhesive pad, its one side was self-glued on the bottom surface of the heat-sink and has low thermal conductivity (1 W/m*K). We cut the TIMs in such a size that it has entirely covered the active area of the CP resistors and the NTC thermistors. In the following sections the superthermal pad is indicated as TIM #1 and the adhesive film as TIM #2. [21]

Finally, in order to improve the thermal behavior of the demonstrator and further cool down the components under up to 40W applied power, we added a DC axial fan (model 2410ML-04W-B39) with plastic casing and blades, used for CPU cooling. Connected to a second power-source, it operates under 12V max. voltage and 0.15A max. current and produces 4000 rpm. It has dimensions 60x60x25 mm (LxWxH) and its blades rotate and circulate the air in front.. [13]

Table 1 summarizes the different components and materials used, based on the data sheets of the components. [13, 14, 15, 21, 22]

Table 1 List of the components of the thermal demonstrator.

Components	Materials
CP power chip resistors	Ni (electrodes) alumina (body)
Multilayer NTC thermistors	Ni (electrodes) alumina (body)
DC axial Fan	plastic (casing and blades)
TIM #1	superthermal gap filler pad
TIM #2	adhesive film
Heat-sink	Al
PCB board	Cu (lines) FR-4 (insulating layer)

Figure 5 shows how the high-power demonstrator looked like after the implementation of the heat-sink, TIMs and DC axial fan while Figure 6 shows the direction of air flow produced by the fan.

Fig. 5 The thermal demonstrator after the heat-sink, TIMs (are placed between the resistors and the heat-sink) and axial fan (can be seen behind the heat-sink) are added to the system.

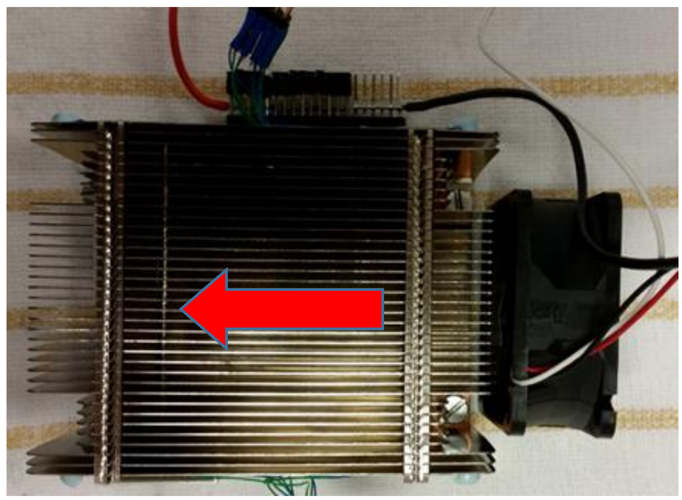

Fig. 6 The red arrow indicates the direction of flow of the air, circulated by the fan attached to the thermal demonstrator

Laboratory setup and software programs used for the measurements and simulations

The power supply sources connected to the system are the 'TOE 8721' and 'TOE 8751', both manufactured by 'TOLLNER'. The first is connected to the fan and the second to the PCB board; by adjusting the V and A buttons (power P = voltage V * current I), the rotational speed of the fan is adjusted and the desired power is produced by the power-source and subsequently is equally distributed to the 14 CP resistors, which are the heat-sources of the system, as described above. [13, 16-17]

A standard digital multimeter was connected to the pins of the PCB, one of each leads to each of the 13 NTC thermistors of the system. As described above, they are the reference elements for the comparison of the temperature values obtained during the experimental measurements and simulations. Based on the power applied, the electrical resistance of each NTC measured and the different temperature values were extracted, based on the R-T data sheet given by the manufacturer. [14-17]

The software tools used for the design of the PCB board, thermistors, resistors, heat-sink and TIMs are the following: Xpedition Enterprise, KLayout, Solidworks and COMSOL Multiphysics. Subsequently for the different cases of simulations we the COMSOL software program. The softwares are installed on one of the servers of the Fraunhofer EAS Institute, which has the following characteristics: Intel (R) Xeon (R) CPU @ 2.90 GHz (2 Processors), 256 GB RAM, running on Windows server 2008 R2 Enterprise (64-bit).

Boundary conditions applied

The following section describes the boundary conditions used during the various simulation cases. For the first set of simulation (before the implementation of the cooling solutions) the 'heat transfer in solids' module of COMSOL Multiphysics was selected. The mechanism that describes the heat dissipation and distribution through the components of the system is the natural convection mechanism. For the second part of the simulation a combination of 'heat transfer in fluids' and 'heat transfer in solids' modules were implemented, in order to simulated the airflow produced by the DC axial fan.

The most important material property for the simulations is the thermal conductivity; it describes the ability of the material to dissipate the applied heat. Other important material properties are the heat capacity C_p and the material density ρ. Additionally, the convective heat transfer coefficient $h_{c,}$ the ambient temperature T_{ext} and the rate of heat transfer Q need to be given, in order to define the how the natural convection heat transfer mechanism works. The h_c parameter was set to 3 W/m^2*K, the ambient (external) temperature was 22 °C and Q is automatically calculated by COMSOL software based on the equation: $Q=h_c*(T_{ext}-T)$. Finally, the applied power (expressed in W) was given during the simulations. In all cases, the 14 CP power resistors were selected as the heat-sources.

The numerical values of the thermal conductivity are automatically set by the material library of COMSOL. We changed the k parameter for the two TIMs implemented, based on the data sheets of their manufacturers. Table 2 summarizes all the numerical values of the k used.

Table 2 The numerical values of the thermal conductivity k of materials in the thermal demonstrator.

Material	Thermal conductivity k [W/m*K]
Cu	400
Ni	90.7
TIM #1	8.9
TIM #2	1
FR-4	0.3
Alumina	27
Aluminum	238

Concerning the mesh options used, we implemented the 'fine mesh' option of COMSOL. The minimum element size applied is 0.424 mm and the maximum element size is 5.83 mm.

Figure 7 shows the array of the CP power heat-sources used during simulations. Next to each NTC of the system, a number appears; their enumeration will be extensively used in the following section of the article, where we present the temperature variation for each NTC thermistors under the applied power.

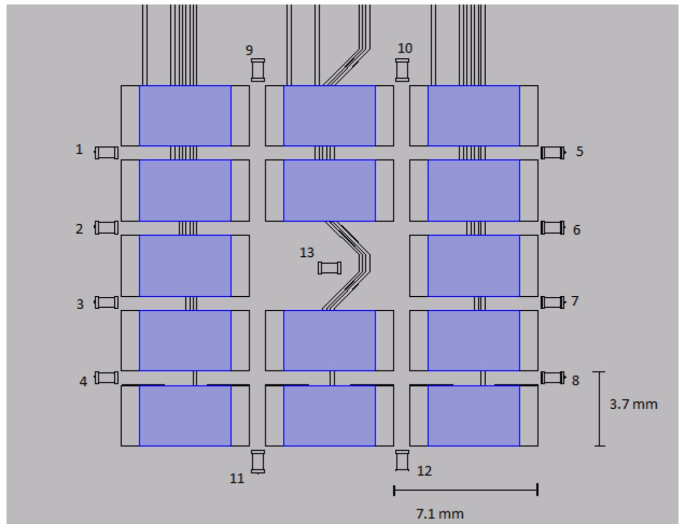

Fig. 7 The blue blocks show the CP power resistors used as heat-sources for the system. Every NTC thermistor is enumerated.

For the simulations that include the T-reduction components, an air block around the system was designed; it emulates the air flow produced by the fan and distributed through the system and the fins of the heat-sink. As shown on figure 6 the fan is placed next to the demonstrator and the air flows from right to left. The exact air movement was simulated with COMSOL Multiphysics; the airflow under 12V/0.15A is 0.54 m^3/min, as indicated in the data sheet. [13]

Figure 8 shows the modeled version of the test-demonstrator after the heat-sink and the two TIMs are added.

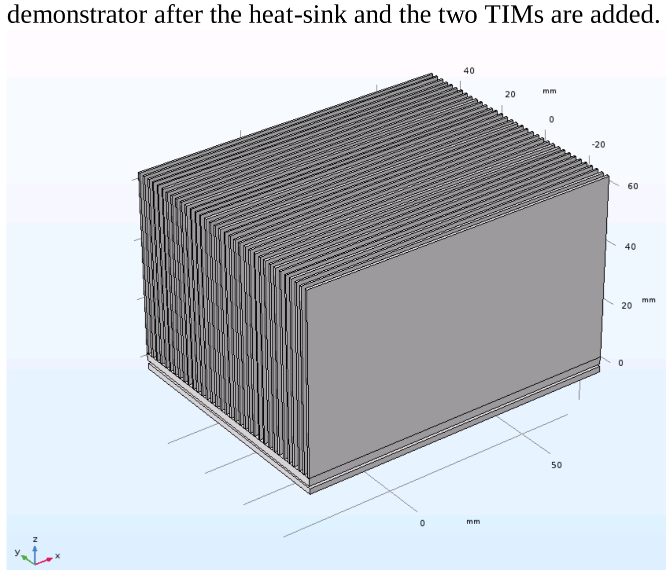

Fig. 8 Modeled version of the thermal demonstrator after the TIMs and heat-sink are added

SIMULATIONS, MEASUREMENTS AND RESULTS

After describing the system components, parameters and boundary conditions, and external equipment connected to the thermal demonstrator, the following chapter of the publication describes the thermal performance and behavior of the system with respect to the results obtained after the simulations and the experimental measurements. The first part compares the numerical results between the simulations and the experimental measurements before the implementation of the heat-sink, TIMs and fan starting from 0W and room temperature and going up to 7W. The second part describes the same comparison after the addition of these features, starting from room temperature and 0W of applied power and driving the system up to approximately 40W.

At the end of the chapter, based on the graphs and equations (extracted during the experimental measurements) that describe the R-T relation for each NTC of the demonstrator, we try to predict the thermal behavior of the system under 50W and 100W of applied power with the cooling mechanisms included. As mentioned in other sections, the temperature values of the 13 NTCs are used for the comparison.

Even though the use of embedded temperature sensors inside the power sources could have shown the maximum temperature values of the CP components and hence of the system, for our simulations and measurements we used the NTCs thermistors instead. Due to the fact that they are placed adjacent to the CP power resistors, they don’t show the same temperature values with them. However, the purpose of the simulations and measurements conducted on the thermal demonstrator was not to extract the maximum temperature values of the system, but to show how it behaves and how the thermal profile of the system changes if the aforementioned temperature-reduction components and solutions are implemented. For that purpose, a big emphasis is given on the temperature values inside each NTC, since their use as reference components reduces the degree of the system complexity. More specifically we are interested in investigating in what degree the temperature values of the NTCs are decreased after the incorporation of the two TIMS, the copper heat-sink and the fan, if different power values up to 35W are applied.

Simulations-measurements comparison prior to the implementation of the cooling features

Starting the measurements with any power being applied and at room temperature (~22 ºC), we measured the R-values for all the NTCs using the digital multimeter. Based on the R-T relation given by their manufacturer, we calculated the temperature inside each NTC; the same methodology was followed through all the measurements. Subsequently we increased the overall applied power by 1W each time. Under 7W the NTCs exhibited very high temperatures (e.g 164 ºC for the central NTC #13) and thus no further power increase was applied.

Table 3 shows the comparison of the T-values of the 13 NTCs of the system under 7W applied power. The percentages in the parentheses in the right column show the % difference for the temperature values extracted between the experimental results and the simulations.

Table 3 Comparison between the temperature values obtained during simulations and measurements for the 13 NTCs of the demonstrator under 7W of applied power.

Selected NTC thermistor	Temperature [°C] (simulations)	Temperature [°C] (measurements)	
1	85.4	85.0	(0.5%)
2	89.2	88.7	(0.6%)
3	88.3	86.8	(1.7%)
4	88.8	87.5	(1.5%)
5	106.1	108.6	(2.3%)
6	110.5	113.0	(2.2%)
7	109.2	112.1	(2.6%)
8	104.6	107.0	(2.2%)
9	118.8	121.9	(2.5%)
10	122	125.9	(3.1%)
11	107.1	109.4	(2.1%)
12	104.8	107.8	(2.8%)
13	157.4	164.2	(4.1%)

Based on table 3, we observe that we achieved a very good numerical proximity for the T-values between the simulations and the actual measurements for all the NTCs of the test-system. The central NTC thermistor (#13) shows the highest deviation (4.1%) between simulations-measurements. This is a normal result, since the simulations cannot fully represent the same conditions applied during the experimental measurements. The thermistor #13 shows the highest T-value amongst all the NTCs (with T~ 164 ºC). The heat density in the middle area of the board is more intense that in the other parts of it.

Figure 9 shows the temperature distribution of the system under 7W of applied power. Based on COMSOL Multiphysics, the simulation time for all the different simulations conducted was between 70-90 seconds. The maximum temperature in the demonstrator can be observed in the CP power resistors, a fact that is absolutely reasonable, since they are the heat-sources of the system.

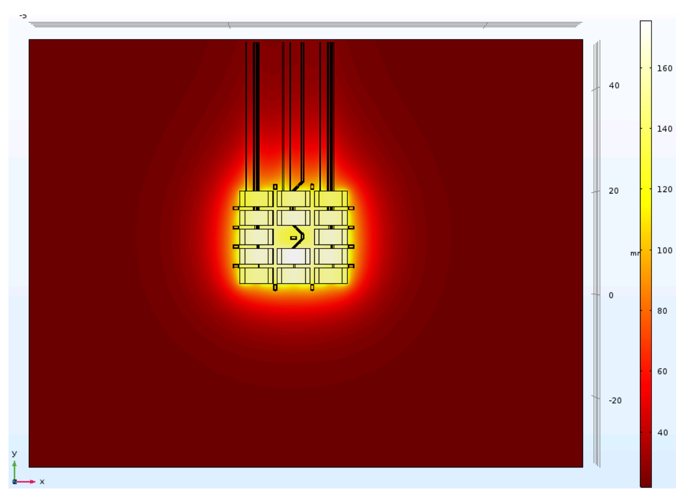

Fig. 9 Thermal profile of the demonstrator under 7W of applied power. The T_{max} is approx.. 173 ºC.

Figure 10 is a Power-T graph, with the x-axis representing the power applied (0-7W, 1 W step) on the demonstrator during the measurements and the y-axis showing the T-range.

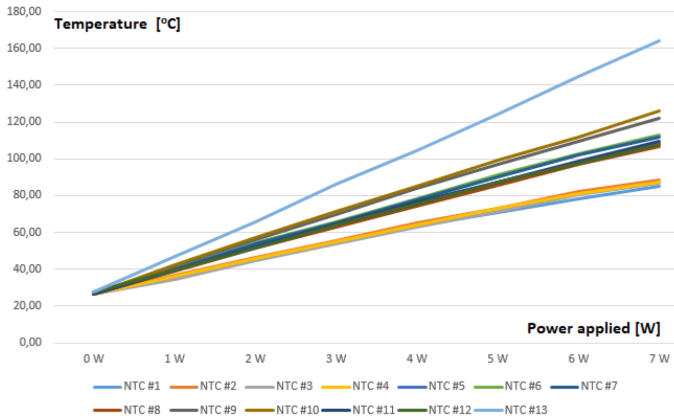

Fig. 10 The Power-Temperature graph shows how the temperature of the 13 NTCs linearly increases under 0-7W applied power (with 1W step). Each thermistor is represented by an unique colored line.

Simulations-measurements comparison after the implementation of the cooling features

The second part of the chapter is dedicated to the results we obtained during the simulations and experimental measurements after the addition of the two TIMs, heat-sink and axial DC fan to the thermal system. The same methodology is followed, as described in the first part of the chapter: we compare the temperature values between the simulations and the experiments for all the NTC thermistors of the demonstrator for 0-35W applied power this time, with 5W step. The 39W was the highest value of power the power-source could supply, but during the experiments we used the 0-35W range. The simulation time for the new simulations was approx. 18-20 minutes due to the new geometries and boundary conditions added to the system. At the end of the chapter we present and describe how the thermal system (with the T-reduction components included) is expected to behave if the applied power is 50W and 100W.

Table 4 presents the comparison between simulations-measurements for the T-values of the NTCs under 35W of applied power. The percentages in the parentheses show the % difference for the values obtained during the experimental measurements and the simulations.

Table 4 Comparison between the temperature values obtained during simulations and measurements for all the NTCs of the demonstrator under 35W of applied power after the implementation of the T-reduction components.

Selected NTC thermistor	Temperature [°C] (simulations)	Temperature [°C] (measurements)	
1	41.1	38.4	(7%)
2	41.3	38.9	(6.2%)
3	40.8	37.1	(10%)
4	41.5	39.7	(4.5%)
5	44.6	43.2	(3.2%)
6	44	44.5	(1.1%)
7	44.1	45.2	(2.4%)
8	43.3	44.6	(2.9%)
9	44.4	46.3	(4.1%)
10	44.6	42.8	(4.2%)
11	44.3	46.3	(4.3%)
12	43.9	44.8	(2%)
13	44.7	60.9	(26.6%)

According to the results presented in table 4, the temperature values between the simulations and the actual measurements show a small variation for almost all the NTCs of the system, expect the central thermistor #13; its numerical deviation is approximately 26,6%. This can be explained if we take into consideration the fact that the simulations show a uniform heat dissipation from the CP resistors through the TIMs and heat-sink. However, the central area of the board, where the NTC #13 is found is much warmer and the air cannot circulate in such manner as it is depicted in the simulated model of the demonstrator.

Figure 11 shows the temperature distribution in the resistor/thermistor area of the PCB board under 35W of applied power. Due to the very good heat dissipation through the TIMs and the heat-sink, the system is able to show a very good thermal profile. The figure demonstrates the temperature values inside the heat-sources of the demonstrator. According to the chromatic scale the maximum temperature in the system is approximately 71 ºC. However, all the 14 CP power-sources show more or less the same maximum temperature; their central areas (shown in dark red) have T-values around 71 ºC.

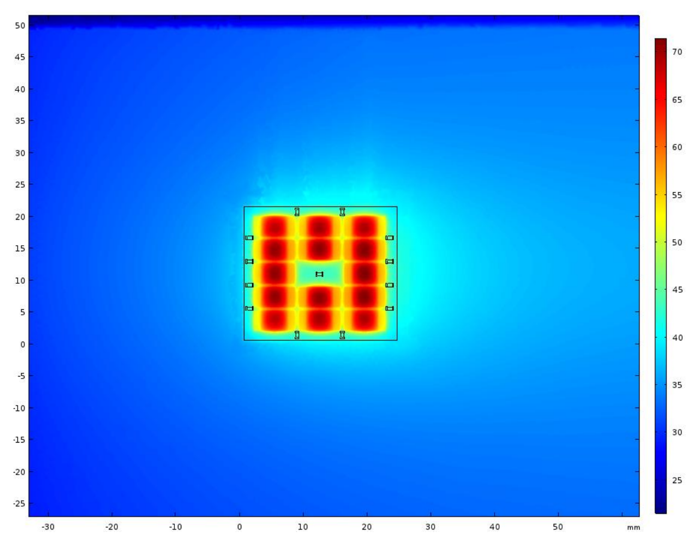

Fig. 11 Temperature distribution of the model under 35W of applied power. The maximum temperature of the system is approximately 71 ºC (in the CP power resistors).

Figure 12 presents in graph how the temperature in each thermistor increases under 0- 35W applied power, with 5 W step). The x-axis shows the power applied during the measurements and the y-axis the temperature range (22-62 ºC). Each NTC of the thermal demonstrator is represented by an unique colored line. Based on the graph, we can observe that the Power-Temperature relationship is approximately linear.

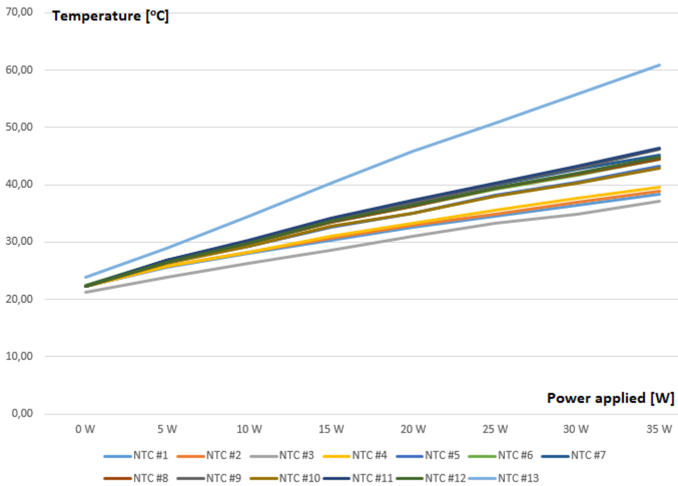

Fig. 12 The Power-Temperature graph shows how the temperature of the thermistors increases if the applied power is increased by 5W each time (during the conduction of the experimental measurements).

Based on the numerical constant calculated for the average temperature increase in ºC per 5W of applied power for each thermistor, we calculated the expected temperature values of the thermistors under 50W and 100W. The NTCs are expected to cover a temperature range between 43.7-76.9 ºC (the latter is the temperature expected for the central thermistor #13) under 50W and 65.8-130.3 ºC (for NTC #13) under 100W. Thus, we observe that by adding the two TIMs, the fan and the copper heat-sink, we managed to achieve with a very good thermal behavior and performance in the system; the expected temperature values of all the NTCs (except the central one) will be below 100 ºC for applications under 100 W.

Table 5 shows the expected temperature values for each NTC of the demonstrator for applications under 50W and 100 W power. For example, 3.29 ºC/5W for NTC #9 means that the average increase of the thermistor temperature is approximately 3.3 ºC each time we increase the applied power by 5W.

Table 5 Expected temperature values for the NTCs of the thermal demonstrator under 50W and 100W power.

Selected NTC thermistor	Temper. increase/5 W applied power [ºC/5W]	Expected temper. [°C] under 50 W	Expected temper. [°C] under 100 W
1	2.13	44.8	66.2
2	2.19	45.5	67.4
3	2.21	43.7	65.8
4	2.32	46.6	69.8
5	2.80	51.6	79.6
6	2.95	53.4	82.9
7	3.06	54.4	85.0
8	2.99	53.5	83.5
9	3.26	56.0	88.6
10	2.75	51.1	78.6
11	3.25	56.1	88.6
12	3.04	54.0	84.4
13	5.33	76.9	130.3

Summary & Conclusions

In this publication we presented, modeled, simulated and investigated the thermal behavior and performance of a high-power microelectronic thermal demonstrator, whose main components are several NTC thermistors and several CP series power resistors, mounted on a standard PCB board.

After we described the structure of the demonstrator, its various components, the experimental and software setup used for the experiments and various simulation cases, the details and the boundary conditions of the model used during the simulations, we presented the thermal behavior of the system before and after implementing several temperature-reduction components. They are essential elements added to the thermal demonstrator in order to reduce its thermal behavior and improve its heat dissipation and distribution under approximately 40W of applied power. For that purpose, a heat-sink, two different TIMs and a DC axial fan were added to the system.

Before the insertion of these T-reduction elements, the system exhibited very high temperature values up to 173 ºC under 7W of applied power. Moreover, based on the comparison of the temperature values between the simulations and the experimental measurements under 7W of applied power, a very good numerical proximity for the T-values of the 13 NTC thermistors was achieved.

Subsequently, by adding an aluminum heat-sink, two TIMs and a fan used for CPU cooling to the demonstrator, we ensured that due to the excellent thermal properties of the TIMs and aluminum, the major part of heat was dissipated through the heat-sink and the air. Additionally, we managed to significantly improve the overall thermal behavior of the system and reduce the overall temperatures of the system's components: under 35W of applied power the maximum temperature of the system was approximately to 71 ºC (in the CP power resistors) and the temperature in the NTCs was not higher than 61 ºC.

An improved thermal performance means better stability, enhanced reliability and robustness for the thermal demonstrator. These factors were ensured in the present case, since during the conduction of the experiments the test-system was able to function perfectly for many hours without any troubleshoot.

Finally, based on the linear equation that gives the power-temperature relationship calculated for each NTC thermistor, we tried to predict what temperature values the NTCs of thermal demonstrator will expect to demonstrate under 50W and 100W of applied power. Under 50 W temperature values up to 66 ºC are expected for the NTCs of the system, while under 100 W the NTCs of the demonstrator expect to have temperature values below 100 ºC except of the central thermistor.

Acknowledgments

This work has been funded within the project SiPoB-3D under label 16ES0384 by the German Ministry of Education and Research (BMBF = Bundesministerium für Bildung und Foschung). Furthermore, it was supported by the Fraunhofer Internal Program SmartTicket under Grant No. MAVO 828 440.

References

[1] W. J. Plumbridge, R. J. Matela, A. Westwater, 'Structural Integrity and Reliability in Electronics', p. 275-286, Springer, 2003

[2] B.Banafsheh et al. 'Multiscale Transient Thermal Analysis of Microelectronics', J. Electron. Packag. 137(3), 031002 (Sep. 2015)

[3] Heinig, A. et al. (2014) ‘Thermal analysis and optimization of 2.5D and 3D integrated systems with wide I/O memory’. Springer.

[4] Lau, John (1993) ‘Thermal Stress and Strain in Microelectronics Packaging’, ISBN 978-1-4684-7767-2, Springer.

[5] Kaiçar Ammous, Slim Abid, Anis Ammous, (2007) "Thermal modeling of semiconductor devices in power modules", Microelectronics International, Vol. 24 Issue: 3, pp.46-54, https://doi.org/10.1108/13565360710779190

[6] A. Heinig, D. Papaioannou, R. Fischbach, ‘Model abstraction of 3D-integrated/interposer-based high performance systems for faster (thermal) simulation’, 2016 15th IEEE Intersociety Conference on Thermal and Thermomechanical Phenomena in Electronic Systems (ITherm), Las Vegas, NV, 2016, pp. 230-237

[7] A. Heinig, D. Papaioannou, R. Fischbach, ‘Thermal considerations for systems with high speed memories’, 2015 European Microelectronics Packaging Conference (EMPC), Friedrichshafen, 2015, pp. 1-6

[8] P. Rodges, V. Eveloy, 'Prediction of Microelectronics Thermal Behavior in Electronic Equipment: Status, Challenges and Future Requirements', IEEE Transactions on Components and Packaging Technologies, volume: 28, issue: 4, Dec. 2005, pages 817-829, DOI: 10.4071/1551-4897-1.1.16

[9] A. Heinig, D. Papaioannou, ‘Comparison between thermal simulations and experimental measurements on an advanced microelectronics test-system’, 2017 16th IEEE Intersociety Conference on Thermal and Thermomechanical Phenomena in Electronic Systems (ITherm), Orlando, Florida, USA, 2017, pp. 428-435

[10] Rodgers, Peter & Eveloy, Valerie. (2004). Prediction of Microelectronics Thermal Behavior in Electronic Equipment: Status, Challenges and Future Requirements. Journal of Microelectronics and Electronic Packaging. 1. . 10.4071/1551-4897-1.1.16.

[11] ‘Heat sink selection methodology in cooling electronics’, QPedia, Advanced Thermal Solutions Inc., 2010

[12] K. Chung ‘Effective thermal management with different thermal interface materials for different applications’, AI technology Inc., 2012

[13] ‘DC Axial Fans - 2410ML-04W-B39’ datasheet: http://www.nmbtc.com/content/pdfs/2410ML.pdf

[14] Susumu Chip Power Resistor CP series datasheet: http://www.mouser.com/ds/2/392/susumu_products_14-609841.pdf

[15] Panasonic NTC Thermistor datasheet: https://www.mouser.de/ProductDetail/Panasonic/ERT-J1VA220J/?qs=%2fha2pyFadujT3yVslHftO9EL2FhbxohOJdy8MYwHYqQBJXrxrdqzLg==

[16] ‘TOELLNER TOE 8721’ power-source datasheet: http://www.toellner.de/html/img/pool/DE_8721_22.PDF

[17] ‘TOELLNER TOE 8751’ power-source datasheet: http://skye-electronics.com/product/toellner-toe-8751-16/

[18] COMSOL Multiphysics ver 5.1 ‘Free Convection in a Water Glass’ example http://www.comsol.com/model/download/227291/models.heat.cold_water_glass.pdf

[19] COMSOL Multiphysics ver 5.1 material library https://www.comsol.com/material-library

[20] COMSOL Multiphysics Heat Transfer Module http://hpc.mtech.edu/comsol/pdf/Heat_Transfer_Module/HeatTransferModuleUsersGuide.pdf

[21] ‘Aavid Thermal Interface SuperThermal D089 Gap Filler Pad’ datasheet: http://www.aavid.eu/sites/default/files/products/interface/Aavid_SuperThermal_Datasheet_A01_July2015.pdf

[22] ‘DYNATRON R23’ heat-sink datasheet: https://www.newegg.com/Product/Product.aspx?Item=9SIAB944HR6038